



Optimal shielding thickness for galactic cosmic ray environments



Tony C. Slaba^{a,*}, Amir A. Bahadori^b, Brandon D. Reddell^c, Robert C. Singleterry^a,
Martha S. Cloudsley^a, Steve R. Blattnig^a

^aNASA Langley Research Center, Hampton VA 23681, USA

^bKansas State University, Manhattan KS 66506, USA

^cNASA Johnson Space Center, Houston, TX 77004, USA

ARTICLE INFO

Article history:

Received 16 November 2016

Revised 21 December 2016

Accepted 21 December 2016

Keywords:

Space radiation
Radiation shielding
Radiation transport
HZETRN
Geant4
FLUKA
PHITS
MCNP6

ABSTRACT

Models have been extensively used in the past to evaluate and develop material optimization and shield design strategies for astronauts exposed to galactic cosmic rays (GCR) on long duration missions. A persistent conclusion from many of these studies was that passive shielding strategies are inefficient at reducing astronaut exposure levels and the mass required to significantly reduce the exposure is infeasible, given launch and associated cost constraints. An important assumption of this paradigm is that adding shielding mass does not substantially increase astronaut exposure levels. Recent studies with HZETRN have suggested, however, that dose equivalent values actually increase beyond $\sim 20 \text{ g/cm}^2$ of aluminum shielding, primarily as a result of neutron build-up in the shielding geometry. In this work, various Monte Carlo (MC) codes and 3DHZETRN are evaluated in slab geometry to verify the existence of a local minimum in the dose equivalent versus aluminum thickness curve near 20 g/cm^2 . The same codes are also evaluated in polyethylene shielding, where no local minimum is observed, to provide a comparison between the two materials. Results are presented so that the physical interactions driving build-up in dose equivalent values can be easily observed and explained. Variation of transport model results for light ions ($Z \leq 2$) and neutron-induced target fragments, which contribute significantly to dose equivalent for thick shielding, is also highlighted and indicates that significant uncertainties are still present in the models for some particles. The 3DHZETRN code is then further evaluated over a range of related slab geometries to draw closer connection to more realistic scenarios. Future work will examine these related geometries in more detail.

Published by Elsevier Ltd on behalf of The Committee on Space Research (COSPAR).

1. Introduction

For long duration missions in deep space beyond the Earth's magnetic field, prolonged exposure to galactic cosmic rays (GCR) presents a serious health risk to astronauts (NCRP, 2006; NRC, 2006). In order to mitigate the exposure and health risks for astronauts on such missions, shielding strategies have been extensively studied with a focus on material characterization (e.g. effectiveness of polyethylene compared to aluminum) and shielding mass requirements (e.g. exposure versus shield thickness curves) (Wilson et al., 1997; Cucinotta et al., 2006). These studies helped form the current GCR shield design paradigm that passive shielding strategies are inefficient at reducing astronaut exposure levels, and the mass required to appreciably reduce the exposure is impractical within modern launch and cost constraints (Durante and Cucinotta, 2011; Singleterry, 2013). Notably, an implicit assumption

of this paradigm is that adding parasitic shielding mass will necessarily decrease, not increase, astronaut exposure levels.

However, recent studies utilizing an updated version of the deterministic space radiation transport code HZETRN, accounting for neutron backscatter (Slaba et al., 2010) and the pion, muon, and electromagnetic cascade components (Norman et al., 2013a), have suggested that GCR-induced dose equivalent values initially decline over the first 20 g/cm^2 of aluminum shielding and then increase substantially, revealing a previously unobserved local minimum in the exposure versus aluminum thickness curve (Slaba et al., 2013a). Independently, Matthia et al. (2013) found qualitatively similar results in slab geometry exposed to low Earth orbit boundary conditions using Monte Carlo (MC) simulations. If such a result can be verified and validated, the long-held GCR shielding paradigm could be substantially altered leading to revised optimization strategies for future deep space vehicles and habitats. The identification of an optimal range of shield thicknesses would provide a useful constraint for vehicle design and optimization studies and place added emphasis on material development. It should be noted that in fully equipped vehicles and habitats, a moderate fraction of the material

* Corresponding author. 2 West Reid St., Mail stop 188E, Hampton, VA 23681-2199.

E-mail address: tony.c.slaba@nasa.gov (T.C. Slaba).

thicknesses traversed from the outer boundary to a given location can exceed several hundred g/cm^2 . Therefore, examination of exposures beyond $20 \text{ g}/\text{cm}^2$ of shielding is highly relevant to current and future vehicle design (Norbury and Slaba, 2014).

In this work, the three-dimensional (3D) version of HZETRN (Wilson et al., 2014, 2015a) and four MC transport codes (Geant4 (Agostinelli et al., 2003), FLUKA (Ferrari et al., 2005), PHITS (Sato et al., 2013), and MCNP6 (Goorley, 2014)) are used to verify that a local minimum in the dose equivalent versus aluminum thickness curve occurs near $20 \text{ g}/\text{cm}^2$ for GCR environments. The same models are also evaluated in polyethylene shielding to demonstrate how material selection can significantly alter exposure estimates beyond $20 \text{ g}/\text{cm}^2$. The 3DHZETRN and MC total dose equivalent values are broken down into various components to establish neutron and light ion ($Z \leq 2$) production as the dominant physical interactions leading to build-up in dose equivalent values beyond the local minimum in aluminum. It is also shown that significant uncertainties remain in the underlying nuclear physics models for light ion production leading to relative variation in model results for total dose equivalent on the order of 30% at $100 \text{ g}/\text{cm}^2$ of aluminum. Much larger variation is observed on individual particle energy spectra for ^2H , ^3H , and ^3He . A similar finding was also shown in a recent study comparing transport code results to Mars Science Laboratory Radiation Assessment Detector (MSL/RAD) particle spectra measurements from the Mars surface (Matthia et al., 2016). The shielding analysis results presented herein further highlight the importance of rigorously quantifying and reducing neutron and light ion physics uncertainties given the potential impact on future vehicle design and optimization.

Finally, the slab geometry chosen for this first set of comparisons utilizes infinite lateral dimensions so that leakage is restricted to the front and back surfaces, thereby placing a reasonable upper bound on the demonstrated build-up effects. In more realistic geometry, and even simplified spherical geometry, leakage will occur from all bounding surfaces and could potentially modify the qualitative trends found in the idealized slabs considered here. For astronaut exposure and risk calculations, moderate tissue self-shielding will further alter the slab results due to the efficiency of hydrogen in attenuating low energy neutrons. In order to gauge the impact of these effects, the 3DHZETRN code is used to evaluate dose equivalent within modified slab con with varying lateral dimensions and water absorber thicknesses.

Future work will examine the effect of leakage and water absorbers on exposure estimates in detail to provide more informative exposure assessments for early phase vehicle design and optimization studies. Although this work is focused on verification and information for preliminary design efforts, experimental measurements of light ion yields through thick targets at ground-based accelerators are also being performed to enable validation and rigorous model uncertainty quantification (Crespo et al., 2015). The experimental design for these thick target measurements also influenced the geometry specification in these comparisons, as will be discussed in the next section.

2. Simulation setup

The simulation setup for this work was chosen to provide useful information for engineering design applications and was also influenced by practical considerations associated with computational resources, research interests focused on neutron and light ion physics, as discussed in the previous section, and the need to connect simulation results to related experimental measurement efforts being performed at ground-based accelerators. This section is focused on describing the rationale for selecting the geometry used in this set of inter-code comparisons. The GCR boundary condition, or external source, used for the calculations is also given.

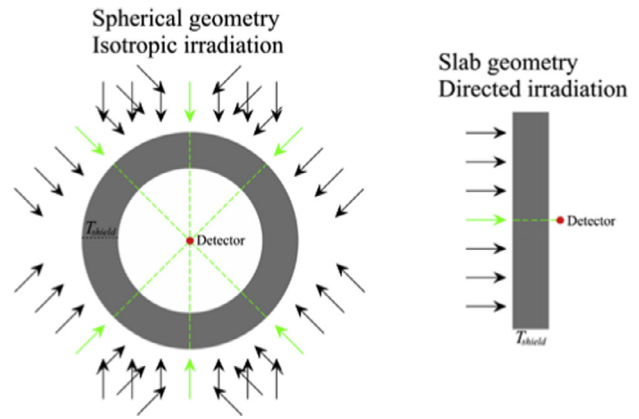


Fig. 1. Spherical geometry exposed to isotropic irradiation (left) and slab geometry exposed to directed radiation (right). The spherical shell and slab thicknesses are $T_{shield} \text{ g}/\text{cm}^2$.

Tallies used in the MC simulations to estimate flux and dose equivalent and their relationship to 3DHZETRN quantities are described in detail in Appendix A.

2.1. Geometry

Early phase vehicle and habitat design studies often consider simplified spherical shielding to facilitate initial trade studies over a broad range of configuration options. Such studies may evaluate exposures versus spherical shield thickness (depth) curves for various candidate shielding materials, thereby allowing preliminary mass requirements and radiation constraints to be balanced against additional mission parameters. The HZETRN code has been used frequently in these engineering applications primarily due to its computational efficiency. However, until very recently (Wilson et al., 2014, 2015a), HZETRN has utilized the straight-ahead approximation to reduce the 3D Boltzmann transport equation to one spatial dimension. For one-dimensional (1D) transport calculations, isotropic irradiation of spherical geometry with a detector located at the center of the sphere is equivalent to uniformly directed irradiation (normal incidence) of slab geometry with a detector placed behind the slab.

Fig. 1 shows a spherical shell geometry with thickness $T_{shield} \text{ g}/\text{cm}^2$ exposed to isotropic irradiation along with the related slab geometry having thickness $T_{shield} \text{ g}/\text{cm}^2$ exposed to uniformly directed irradiation. To improve clarity, only selected directions of the incident isotropic irradiation are shown in the spherical geometry case. If off-axis scattering is neglected, as in 1D versions of HZETRN, transport procedures only need to be evaluated along the green dashed rays passing from the boundary, directly through the shield material and detector. It is then clear from the figure that for 1D straight-ahead transport procedures, each of the incident directions in the spherical geometry case are equivalent to the single slab geometry case with a uniformly directed boundary condition and a point detector.

One would expect differences between the two configurations in Fig. 1 to become apparent when 3D transport procedures or MC simulations, which are inherently 3D, are considered. For example, along each of the green dashed rays in the spherical geometry, one can see that $T_{shield} \text{ g}/\text{cm}^2$ of shielding appears both upstream and downstream of the detector, suggesting that back-scattering may influence the measured radiation field at the detector location. Yet, in most of the slab calculations evaluated in the past, downstream shield thicknesses were not considered, primarily due to the 1D nature of HZETRN which did not account for backscattering. Lateral slab dimensions and distance between the detector and back slab

Download English Version:

<https://daneshyari.com/en/article/5498093>

Download Persian Version:

<https://daneshyari.com/article/5498093>

[Daneshyari.com](https://daneshyari.com)